Controllable subwavelength-ripple and -dot structures on Y $Ba_2Cu_3O_7$ induced by ultrashort laser pulses



2012 Supercond. Sci. Technol. 25 115008

(http://iopscience.iop.org/0953-2048/25/11/115008)

Supercond. Sci. Technol. **25** (2012) 115008 (5pp) doi:10.1088/0953-2048/25/11/115008

# Controllable subwavelength-ripple and -dot structures on $YBa_2Cu_3O_7$ induced by ultrashort laser pulses

**C W Luo[1], W T Tang[1], H I Wang[1], L W Liao[1], H P Lo[1], K H Wu[1], J-Y Lin[2], J Y Juang[1], T M Uen[1] and T Kobayashi[1,3]**

[1] Department of Electrophysics, National Chiao Tung University, Hsinchu, Taiwan, Republic of China
[2] Institute of Physics, National Chiao Tung University, Hsinchu, Taiwan, Republic of China
[3] Advanced Ultrafast Laser Research Center, and Department of Engineering Science, Faculty of Informatics and Engineering, The University of Electro-Communications, Chofugaoka 1-5-1, Chofu, Tokyo 182-8585, Japan

E-mail: cwluo@mail.nctu.edu.tw

Received 30 March 2012, in final form 30 August 2012
Published 19 September 2012
Online at stacks.iop.org/SUST/25/115008

**Abstract**
The evolution of periodic ripples and dots on an $YBa_2Cu_3O_7$ surface irradiated by single-beam and dual-beam femtosecond laser pulses is investigated. The density and size of the dots can be controlled by the number of pulses. The spatial period of these ripples does not show a close relation to the pulse number. However, the orientation and geometrical period of the ripples are strongly dependent on the polarization and incident angle of the laser pulses, respectively. The formation processes are also discussed based on the dependence.

(Some figures may appear in colour only in the online journal)

## 1. Introduction

Since the introduction of femtosecond (fs) laser amplifiers, nanoscale microstructures on the surfaces of materials have been demonstrated by irradiating the surfaces with femtosecond pulses [1–12]. This has attracted a great deal of attention because periodic structures can be inscribed on almost any material directly and without any masks and chemical photoresists to relieve environmental concerns. For instance, nanoripples [1–7], nanoparticles [8–10], nanocones [11] and nanospikes [12] have been induced by single-beam femtosecond laser pulses in various materials. Nowadays, the interference between the surface electromagnetic wave (surface plasmons) and the incident light has been widely accepted to explain the femtosecond laser-induced subwavelength periodic surface structures (LIPSSs) [2–7]. However, studies on the evolution of ripples under irradiation by circularly polarized light and the formation of dot structures are very few. Therefore, the mechanism of their formation has not been further discussed as of yet.

In this paper, we report the formation of ripples and dots on $YBa_2Cu_3O_7$ (YBCO) thin films irradiated by a single-beam and a dual-beam fs laser, respectively. The dependence of the subwavelength ripples on the incident angle and circularly polarized light is obtained. Finally, a physical model in terms of the interference between the surface plasma wave and the incident light is proposed to explain our results.

## 2. Experiments

The YBCO samples used in this study were prepared by pulsed laser deposition with a KrF excimer laser. The growth and characterization of the (001)-oriented YBCO thin films have been discussed in detail elsewhere [10]. Briefly, the thickness of all films on (001) $SrTiO_3$ (STO) substrates was about 240 nm. The $T_c$ of a YBCO thin film is about 89.5 K, as shown in figure 1. Figure 2(a) shows the surface morphology of a typical (001)-oriented YBCO thin film scanned by an ultra-high resolution field emission scanning electron microscope (FEG-SEM, JOEL JSM-7000F). The

 

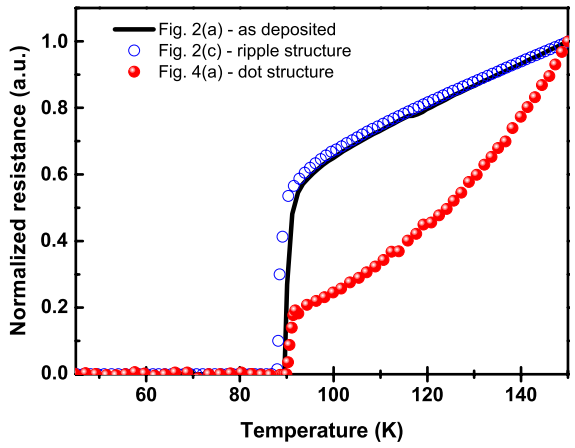


**Figure 1.** The temperature dependence of the normalized resistance for as-deposited YBCO (figure 2(a)), YBCO thin film with a ripple structure (figure 2(c)) and YBCO thin film with a dot structure (figure 4(a)).

surface roughness of an as-deposited YBCO thin film was around 4 nm identified by its AFM image.

A commercial regenerative amplified Ti:sapphire laser (Legend USP, Coherent) with 800 nm wavelength, 80 fs pulse duration, ∼0.5 mJ pulse energy and 5 kHz repetition rate was used as the irradiation source. After passing through a variable neutral density filter and a quarter-wave plate, the normal incident laser beam was focused onto the sample surface with a spot size of ∼200 $\mu$m (FWHM) by a convex lens with 50 mm focal length. The pulse number or irradiation time was precisely controlled by the electric shutter. For the dual-beam scheme, a modified Michelson interferometer was applied to produce the dot structure on YBCO thin films. The polarizations of both beams could be individually controlled by two quarter-wave plates before the reflection mirrors in both arms of the dual-beam setup. After a beam splitter in the dual-beam setup, both beams were collinearly and simultaneously focused on the sample surfaces by a

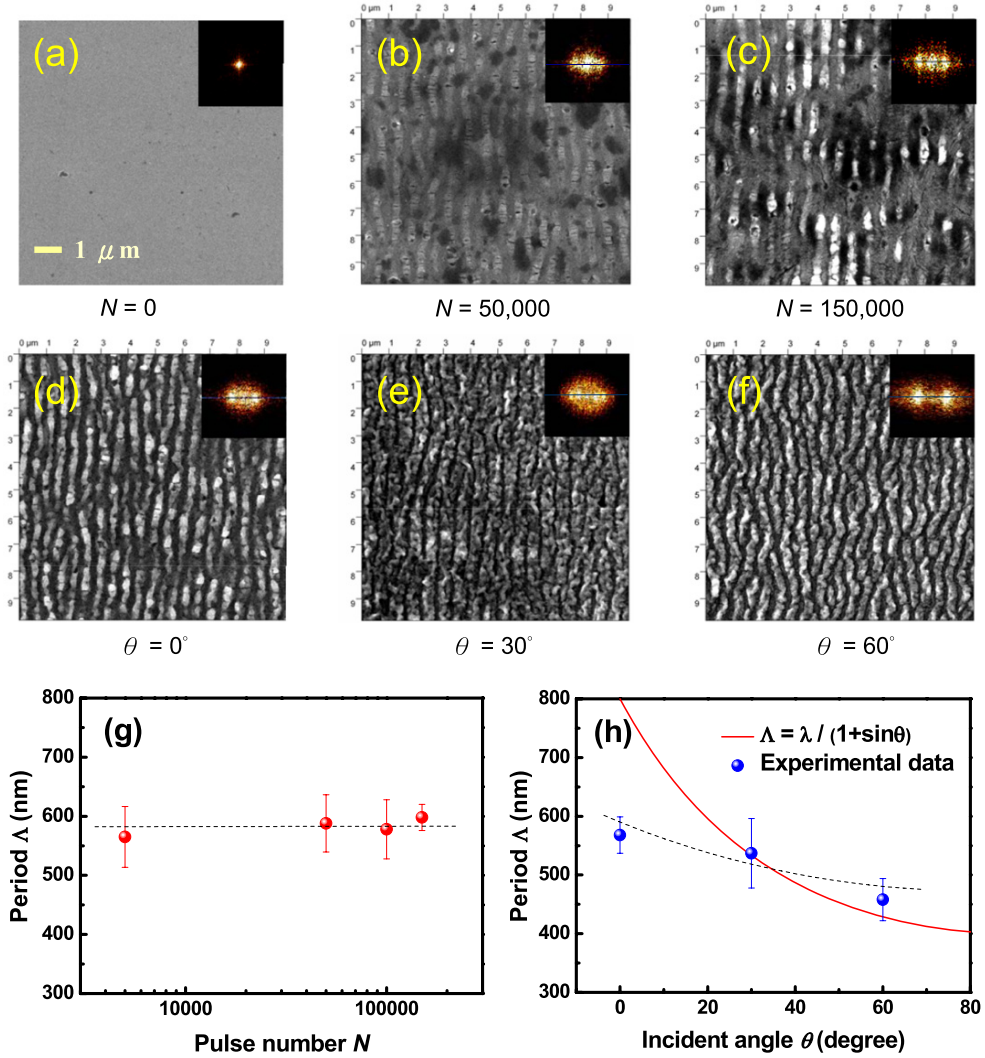


**Figure 2.** (a)–(f) The morphological evolution of structures on YBCO thin films induced by a linear polarized fs laser with various pulse numbers (incident angle = 0°, fixed $F = 75$ mJ cm$^{-2}$) and incident angles ($N = 150\,000$, $F = \sim 300$ mJ cm$^{-2}$). (g) The dependence of the period of the ripples on the pulse number. (h) The dependence of the period of the ripples on the incident angle. Inset: the 2D Fourier spectra which were transferred from their corresponding SEM images (10 $\mu$m × 10 $\mu$m). The scale bar is applied to all figures. The dashed lines are guides to the eyes.

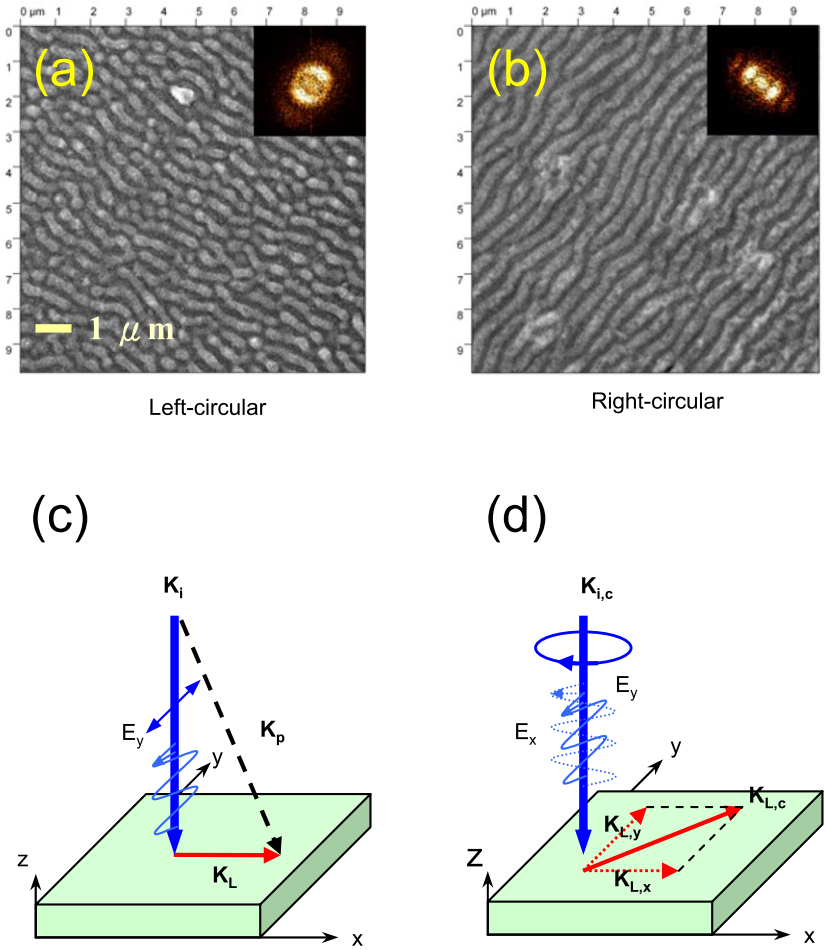


**Figure 3.** The SEM images (10 $\mu$m × 10 $\mu$m) of fs LIPSS induced by (a) the left- and (b) the right-circularly polarized beams. (c) Schematic of the momentum conservation condition for the wavevectors of linear polarized laser light ($K_i$), plasma wave ($K_p$), and LIPSS ($K_L$). (d) Schematic processes of the LIPSS by the circularly polarized laser light ($K_{i,C}$). The scale bar is applied to all figures.

convex lens with 50 mm focal length. All experiments were performed in air under atmospheric pressure.

## 3. Results and discussion

The SEM analysis (figure 2 with a pixel resolution of ∼0.04 nm) indicates that the morphology of fs laser-induced surface structures depends on both the number of applied pulses and the laser incident angle ($\theta$ is the angle of incidence with respect to the surface normal). Figures 2(a)–(c) show the evolution of the ripple structure on YBCO thin films irradiated by a single-beam fs laser with various pulse numbers ($N$) and a fixed fluence ($F$) = 75 mJ cm$^{-2}$ at a fixed incident angle of 0°. On increasing the pulse number, the ripple structure becomes clear in the SEM images, which can be evidenced from the appearance of satellite peaks in the 2D Fourier spectra of the insets of figures 2(b) and (c) (there are no satellite peaks in the inset of figure 2(a) for an as-deposited YBCO thin film). The spatial period of the ripples, estimated from the position of a satellite peak in the 2D Fourier spectra, is independent of the pulse number and irradiation time as shown in figure 2(g). Once the pulse number was greater than or equal to 5000, i.e. the sample surface was irradiated by the 75 mJ cm$^{-2}$ femtosecond laser pulses for 1 s, ripples with a peak-to-valley height of ∼106 nm could be clearly observed on the sample surface. On the other hand, if the fluence and pulse number were, respectively, fixed at ∼300 mJ cm$^{-2}$ and 150 000, we found that the spatial period decreased with increasing incident angle ($\theta$) (see figure 2(h)). However, the observed period of the ripple at $\theta = 0°$ is significantly smaller than the prediction of $\Lambda = \lambda/(1 + \sin\theta)$ [13]. Besides, the incident angle-dependent period of ripples on YBCO thin films cannot be described by this simplified scattering model (the solid line in figure 2(h)). Therefore, the effect of the surface electromagnetic wave, i.e. surface plasmons (SPs), should be taken into account for the formation of subwavelength ripples [2, 7]. According to Shimotsuma *et al*'s results [14], the femtosecond incident light easily excites the plasmons on the surface of various materials. As shown in figure 3(c), once the momentum conservation condition for the wavevectors of the linearly polarized laser light ($K_i$), plasma wave ($K_p$) and LIPSS ($K_L$) is satisfied, such a plasmon could couple with the incident light. The interference between the plasmons and the incident light would generate a periodically modulated electron density to cause the nonuniform melting. After femtosecond laser

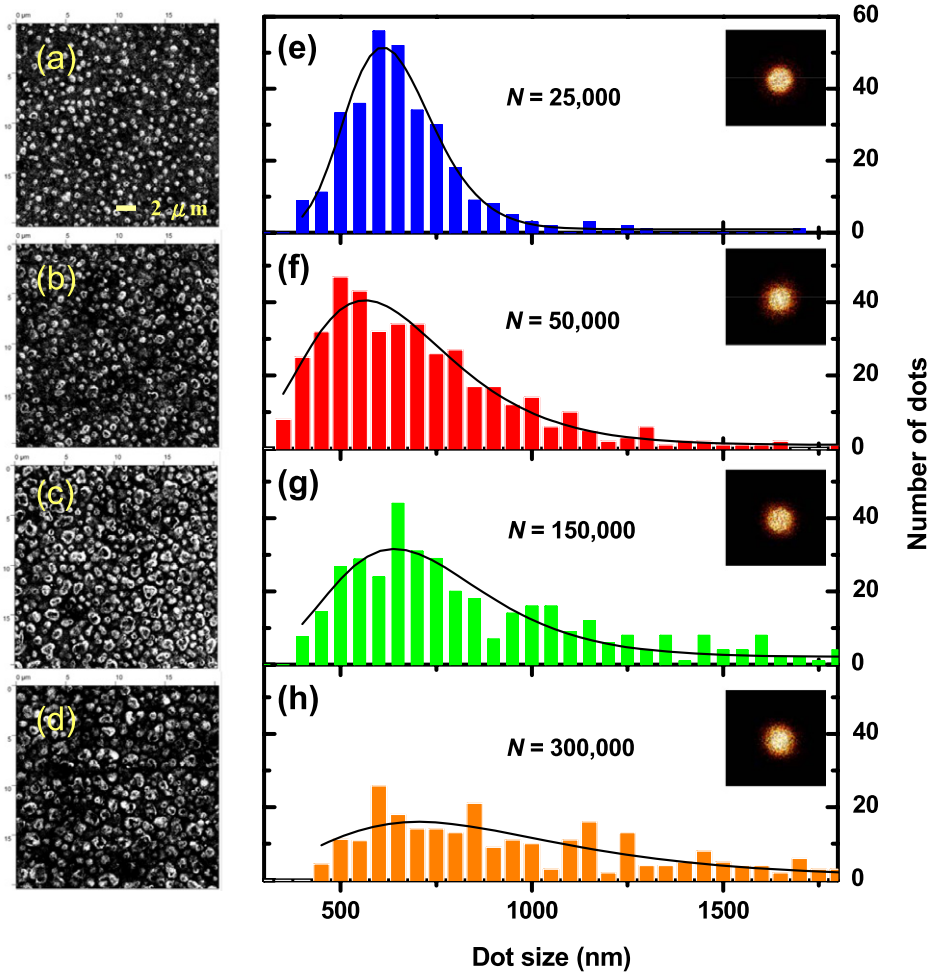


**Figure 4.** (a)–(d) The dot structures on YBCO thin films induced by a dual-beam setup with various pulse numbers ($N$) and a fixed fluence of 87 mJ cm$^{-2}$. (e)–(h) The size distributions correspond to the SEM images (20 $\mu$m × 20 $\mu$m) (a)–(d), respectively. The solid lines are the log-normal fitting. Insets: the 2D Fourier spectra which were transferred from their corresponding SEM images (a)–(d), respectively. The scale bar is applied to all figures.

irradiation, the interference ripple is inscribed on the YBCO surface. Moreover, the superconductivity of the YBCO with the ripple structure in figure 2(c) remained nearly unchanged as shown in figure 1.

Interestingly, when we used a circularly polarized beam, the ripple structure could still be produced, as shown in figures 3(a) and (b). The orientations of the ripples were observed as $-45°$ and $+45°$ for left- and right-circularly polarized beams, respectively, with respect to the incident plane of the beam. For both cases, the spatial period was 491 nm which was produced by the fs laser pulses with fluences of 185 mJ cm$^{-2}$ and a pulse number of 150 000. These results show that the orientation of the ripple structure strongly depends on the polarization state of the incident fs pulses which is consistent with Zhao *et al*'s results on tungsten [12, 15]. In principle, the circularly polarized light ($K_{i,c}$) can be decomposed into two perpendicular linearly polarized light beams ($E_x$ and $E_y$) with retardation of $\lambda/4$ in phase, as shown in figure 3(d). The linearly polarized light beams $E_x$ and $E_y$ can, respectively, induce the LIPSS $K_{L,x}$ and $K_{L,y}$ while the momentum conservation condition in figure 3(c) is satisfied. Thus, both $K_{L,x}$ and $K_{L,y}$ with phase retardation of $\lambda/4$ further cause the $K_{L,c}$ according to the momentum conservation condition of $K_{L,c} = K_{L,x}+K_{L,y}$. The wavevector of LIPSS ($K_{L,c}$) at 45° is completely consistent with the direction of the satellite peaks in the 2D Fourier spectra (the inset of figure 3(a)). Namely, the orientation of ripples is at $-45°$ for the left-circularly polarized beam with respect to the incident plane of the beam. Similarly, the right-circularly polarized beam induces the wavevector of LIPSS ($K_{L,c}$) at $-45°$ according to the momentum conservation condition of $K_{L,c} = -K_{L,x} + K_{L,y}$, which is consistent with the results in figure 3(b).

In order to clarify the above scenario in the formation of ±45° regular ripples induced by circularly polarized beams, a dual-beam setup with perpendicular linear polarizations was applied to produce the LIPSS on YBCO thin films. As shown in figures 4(a)–(d), it is surprising that there are many dots with a height of ∼116 nm rather than regular ripples on the surface of the YBCO thin film. For the case of a dual-beam setup, the $K_{L,x}$ and $K_{L,y}$ without coherence in phase, which are, respectively, induced by two random phase and perpendicular linear-polarization beams ($E_x$ and $E_y$), would not satisfy the momentum conservation of $K_{L,c} = \pm K_{L,x} +$

$K_{L,y}$ and cannot create the $\pm 45^\circ$ wavevector of LIPSS ($K_{L,c}$). Therefore, the $K_{L,x}$ and $K_{L,y}$ which are perpendicular to each other would lead to 2D nonuniform melting and then further aggregate to form randomly distributed dots (see the 2D Fourier spectra in the insets of figures 4(e)–(h)) due to the surface tension. For the case of $N = 25\,000$, the average size of the dots is around 632 nm in diameter estimated by the log-normal fitting as shown in figure 4(e). Additionally, the $T_c$ of YBCO with nanodot structure is almost the same as that of the as-deposited YBCO thin films (see figure 1). If the pulse number is increased, although the average size only slightly increases from 632 to 844 nm, the size distribution markedly broadens (figures 4(f)–(h)). For $N = 300\,000$, the size of a portion of the dots is of the order of micrometers. However, the larger dots will affect the dot densities on the surfaces of YBCO thin films. For instance, the density of dots increases with an increase in pulse number while the pulse number is greater than or equal to 150 000. Once the dots grow large enough to merge with their nearest neighbors and even their next nearest neighbors, the density of dots will significantly shrink, as shown in figure 4(c). Therefore, the size and density of YBCO dots can be controlled by the pulse number of the fs laser.

## 4. Summary

In summary, the surface morphology of YBCO thin films has been systematically studied under single-beam and dual-beam fs laser irradiation. The generation of ripple and dot periodic structures is decided by the applied laser fluences, pulse numbers and laser polarizations; the period and orientation of ripples and even the size and density of dots can be controlled by these parameters. These results may be potentially applied to the manufacture of nanostructure templates for the growth of YBCO thin films and the fabrication of the microwave filter devices with array structures or weak-link Josephson junction arrays.

## Acknowledgments

This work was supported by the National Science Council of Taiwan under grants NSC98-2112-M-009-008-MY3 and NSC96-2923-M-009-001-MY3, and by the MOE ATU Program operated at NCTU.

## References

[1] Hsu E M, Crawford T H R, Tiedje H F and Haugen H K 2007 *Appl. Phys. Lett.* **91** 111102
[2] Sakabe S, Hashida M, Tokita S, Namba S and Okamuro K 2009 *Phys. Rev.* B **79** 033409
[3] Jia X, Jia T Q, Zhang Y, Xiong P X, Feng D H, Sun Z R, Qiu J R and Xu Z Z 2010 *Opt. Lett.* **35** 1248
[4] Yang Y, Yang J, Xue L and Guo Y 2010 *Appl. Phys. Lett.* **97** 141101
[5] Bonse J and Krüger J 2010 *J. Appl. Phys.* **108** 034903
[6] Okamuro K, Hashida M, Miyasaka Y, Ikuta Y, Tokita S and Sakabe S 2010 *Phys. Rev.* B **82** 165417
[7] Huang M, Zhao F, Cheng Y, Xu N and Xu Z 2010 *ACS Nano* **3** 4062
[8] Teng Y, Zhou J, Luo F, Ma Z, Lin G and Qiu J 2010 *Opt. Lett.* **35** 2299
[9] Jia T Q, Zhao F L, Huang M, Chen H X, Qiu J R, Li R X, Xu Z Z and Kuroda H 2006 *Appl. Phys. Lett.* **88** 111117
[10] Luo C W *et al* 2008 *Opt. Express* **16** 20610
[11] Nayak B K, Gupta M C and Kolasinski K W 2008 *Appl. Phys.* A **90** 399
[12] Zhao Q Z, Malzer S and Wang L J 2007 *Opt. Express* **15** 15741
[13] Zhou G, Fauchet P M and Siegman A E 1982 *Phys. Rev.* B **26** 5366
[14] Shimotsuma Y, Kazansky P G, Qiu J and Hirao K 2003 *Phys. Rev. Lett.* **91** 247405
[15] Zhao Q Z, Malzer S and Wang L J 2007 *Opt. Lett.* **32** 1932